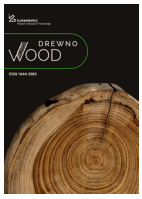
Article citation info:
Icha A.A. 2027. Experimental and Numerical Investigation of Failure Modes and Performance Behaviour of an All-purpose Jig on a Circular Saw Machine. *Drewno. Prace naukowe. Doniesienia. Komunikaty.* https://doi.org/10.53502/wood-215074

Łukasiewicz Poznań Institute of Technology

Drewno. Prace naukowe. Doniesienia. Komunikaty
Wood. Research papers. Reports. Announcements

Journal website: https://drewno-wood.pl



Experimental and Numerical Investigation of Failure Modes and Performance Behaviour of an All-purpose Jig on a Circular Saw Machine

Asibong Asibong Icha*

Department of Wood Products Engineering, University of Cross River State, Calabar, Nigeria

Article info
Received: 19 September 2025
Accepted: 3 December 2025
Published: 26 November 2026

Keywords
all-purpose jig
finite element modelling
circular saw machine
woodworking operations

The need to improve the versatility of circular saw machines, especially in developing countries, remains a top priority. To address this issue, all-purpose jigs have been proposed as a potential solution. Consequently, in this study, an All-purpose Jig (APJ) for circular saw operations was developed and evaluated structurally using both experimental and numerical methods. The APJ allows the circular saw to perform cutting tasks such as tongues, grooves, tenons, and moulding-head returns, while increasing safety and enhancing precision. It consists of a base, vertical fence, carriage/slider, clamp block, and handle. Modelling and simulation were carried out using SolidWorks (2021) to examine von Mises stress, elastic strain, and total deformation. Two materials – medium-density fibreboard (MDF) and African mahogany (Khaya ivorensis) – were considered in the simulation. Following this, a hybrid jig was fabricated by combining mahogany and MDF. The jig was also empirically tested. Simulation results for MDF under a 470 N load showed a maximum von Mises stress of 1.494×10^8 N/m^2, an elastic strain of 2.722×10^1, a deformation of 1.659×10^4 mm, and an FoS of 2, while mahogany under the same load presented a maximum von Mises stress of 1.130×10^7 N/m^2, an elastic strain of 1.338×10^{-4}, a deformation of 0.10^5 mm, and an FoS of 12, confirming its superior strength and rigidity. The APJ offers cost-effectiveness, with an estimated manufacturing cost of US$40.89 as of 2021. The combination of mahogany and MDF demonstrates a practical pathway for optimising structural performance and enhancing safety in woodworking operations.

DOI: 10.53502/wood-215074
This is an open access article under the CC BY 4.0 license:
https://creativecommons.org/licenses/by/4.0/deed.en.

Introduction

Wood machining remains an essential component of the global furniture and construction industries, requiring efficiency, safety and precision (Falko et al., 2023). Among the commonly used machines in wood processing, the circular saw stands out as one of the most versatile yet potentially hazardous (Li et al., 2015; Heisel et al., 2014). To maximise accuracy, reduce operator risk and improve material handling, jigs and fixtures are employed as supplementary devices (Said et al., 2023; Radhwan et al., 2019). A jig is designed to guide the workpiece or cutting tool, enabling repeatable operations and enhancing both productivity and safety (Pethe et al., 2019; Nanthakumar and Prabakaran, 2014). However, despite their widespread use, jigs are often subjected to significant operational stresses and varying load conditions that may compromise their performance and structural integrity (Icha and Odey, 2024; 2025). The development of an APJ – capable of performing different cuts where the stock must be held on its small edge, such as tenons, grooves, tongues, and moulding-head returns – offers great utility but also introduces additional challenges related to load bearing, vibration

* Corresponding author: ichaasibonga@gmail.com

resistance, and long-term durability (Amid et al., 2025; DeCristoforo, 1988; Capototo, 1983). When exposed to cyclic loads during cutting operations, such jigs may undergo failures, including crack initiation, excessive deflection, loosening of fasteners or wear at the interfaces (Radhwan et al., 2019; Okpala and Okechukwu, 2015). Understanding these behaviours is critical, as failure not only reduces productivity but also presents serious safety hazards to machine operators.

Traditionally, investigations into woodworking jigs have been largely empirical, relying on physical prototyping, testing and trial-and-error adjustments (Falko et al., 2023; Miller and Hannam, 1985). While this approach yields valuable practical insights, it is often costly, time-consuming, and limited in its ability to capture the full complexity of the material and structural responses under different conditions (Kumar et al., 2023). Appropriate joint designs are also critical to the final construction durability and strength of these devices (Vassiliou et al., 2016). In recent years, numerical modelling techniques such as the finite element method (FEM) have emerged as powerful tools to complement experimental evaluations (Icha et al., 2024; Marinkovic and Zehn, 2019). FEM enables the simulation of stress distribution, strain localisation and deformation under controlled loading conditions, thus providing predictive insights into how a jig might fail or deform before actual physical failure occurs (Szabó and Babuška, 2021; Marinkovic and Zehn, 2019).

Several studies have demonstrated the usefulness of FEM in analysing woodworking tools and wood-based components. Finite element models have been applied to study wood joints, fracture mechanics and tool–workpiece interactions. Blomqvist et al. (2023) experimentally investigated laminated veneer bending and validated mechanical responses against simulation results. Similarly, Salin (2008) explored water absorption and swelling in wooden members, highlighting environmental factors that may weaken the components. Autengruber et al. (2021) developed a finite-element-based approach to understand the failure mechanics in wood-based composites, showing strong agreement with stiffness predictions. Massaro et al. (2022) validated carpentry joint simulations against experimental results, reporting high prediction accuracy. Huber et al. (2022) employed FEM models integrated with X-ray computed tomography (CT) to recreate structural features in wood, enabling detailed predictions of how grain structure influences failure. Furthermore, Vasis (2025) applied FEM to study crack initiation in wood, emphasising its role in predicting fatigue-related failures. Hu et al. (2022) modelled screw behaviour in wood, while Hong and Barrett (2010) examined nailed connections, both studies highlighting the effect of localised stresses on structural reliability. These studies demonstrate FEM's robustness in modelling complex behaviours of wood, particularly when integrated with real-world data.

In addition, hybrid approaches combining experimental results with numerical simulations have been increasingly recognised as effective in validating theoretical models while also uncovering failure modes that may not be fully captured in simulations alone. Zhong et al. (2012) simulated wood deformation under axial and transverse compression using representative volume elements (RVE) and validated the results with compression tests. Frontini (2023) used FEM to evaluate diaphragm behaviour in wooden roof structures, showing how plank incorporation altered system performance compared with simplified models. Icha and Odey (2022) developed a finite element model of an APJ used with a circular saw machine; the results of their work demonstrated the high predictive accuracy of the simulation. This was complemented by a study on a master jig for a circular saw machine, which demonstrates CAD-driven prototyping and FEM-based simulations (Icha and Odey, 2024; 2025). Despite these advances, there has been only limited research specifically addressing the structural performance and long-term reliability of APJs in circular saw applications, particularly in terms of combined experimental and numerical evaluation to predict critical failure modes.

The integration of experimental and numerical approaches is therefore essential for a more comprehensive understanding of jig performance (Zhong et al., 2021). Experimental tests provide real-world performance data under varying operational conditions such as cutting loads, vibration and feed rate, while FEM simulations allow controlled analysis of stress concentration, displacement patterns and potential points of weakness. Together, they offer a holistic method to investigate failure mechanisms and performance behaviour, guiding improvements in design, material selection and manufacturing practices (Szabó and Babuška, 2021). Given the recent advocacy for the use of jigs in woodworking workshops in Nigeria and the safety-critical nature of their performance, it is important to systematically investigate the failure modes and performance behaviour of APJs using a combined experimental and numerical approach. The research will contribute not only to improving the structural reliability and safety of woodworking jigs, but also to advancing knowledge in the applied mechanics of wood-based tools. It is hypothesised in this study that replacing MDF with African mahogany in the structural components of the all-purpose jig will result in lower deformation, reduced stress concentration, and improved safety margins under operational loads. The findings will also serve as a foundation for more sustainable, durable and safer jig design in the woodworking industries.

Materials and methods

1. Materials

The primary materials employed in this study were medium-density fibreboard (MDF) and African mahogany (*Khaya ivorensis*), sourced from timber suppliers within the research area of Calabar, Nigeria (approximate coordinates: 4.95^0 N, 8.32^0 E). The material was procured as a standard plank from the local wood market and subsequently processed at the University Wood Products Engineering workshop. Fastening components included M10 and M4 end-to-end bolts, each equipped with hand-fabricated knobs to improve ease of use. Additionally, GB recessed CSK wood screws made of steel were utilised to enhance structural integrity. A pictorial view of the fabricated APJ is presented in Fig. 1, while Figs. 2 and 3 contain respectively a detailed drawing and an exploded view of the APJ. The specific configurations and design features of the jig are also outlined in these figures.



Fig. 1. Pictorial view of the designed APJ

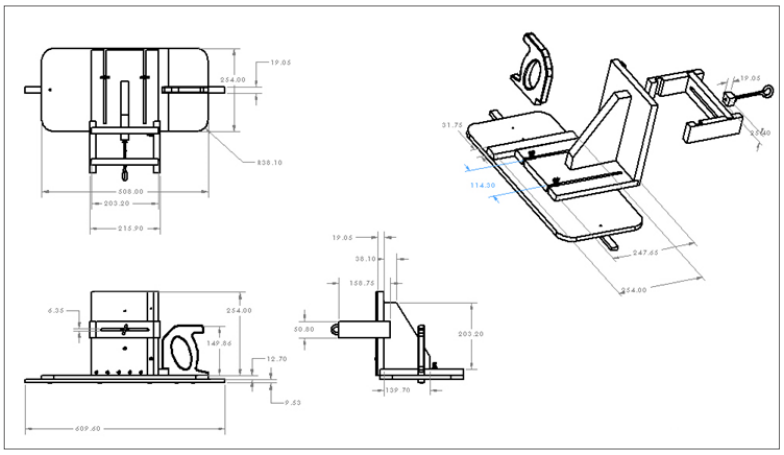
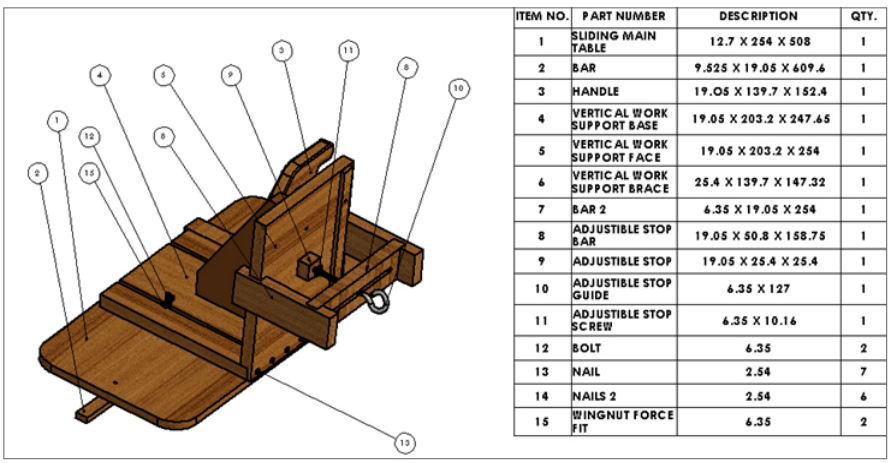


Fig. 2. Detailed drawing of the designed APJ



ITEM NO.	PART NUMBER	DESCRIPTION	QTY.
1	SLIDING MAIN TABLE	12.7 X 254 X 508	1
2	BAR	9.525 X 19.05 X 609.6	1
3	HANDLE	19.05 X 139.7 X 152.4	1
4	VERTIC AL WORK SUPPORT BASE	19.05 X 203.2 X 247.65	1
5	VERTIC AL WORK SUPPORT FACE	19.05 X 203.2 X 254	1
6	VERTIC AL WORK SUPPORT BRACE	25.4 X 139.7 X 147.32	1
7	BAR 2	6.35 X 19.05 X 254	1
8	ADJUSTIBLE STOP BAR	19.05 X 50.8 X 158.75	1
9	ADJUSTIBLE STOP	19.05 X 25.4 X 25.4	1
10	ADJUSTIBLE STOP GUIDE	6.35 X 127	1
11	ADJUSTIBLE STOP SCREW	6.35 X 10.16	1
12	BOLT	6.35	2
13	NAIL	2.54	7
14	NAILS 2	2.54	6
15	WINGNUT FORCE FIT	6.35	2

Fig. 3. Part description of the designed APJ

2. Design considerations

The APJ's design took into consideration fastener resistance, screw-holding capacity, and overall load-bearing performance. The procedures for fastener design were carried out in accordance with the guidelines provided in the Forest Products Laboratory General Technical Report (2010).

2.1. Bolts

The shear and bearing capacity under the bolt were computed using equations (1) and (2) in accordance with Seward (2014).

$$\text{Shear capacity, } F_{v,Rd} = \frac{0.6\, f_{ub} A}{\gamma_{M2}} \quad (1)$$

$$\text{Bearing capacity, } F_{b,Rd} = \frac{f_{ub} dt}{\gamma_{M2}} \quad (2)$$

where: f_{ub} = ultimate tensile strength of bolt, A = bolt tension area/full area, γ_{M2} = partial safety factor = 1.25, d = nominal bolt diameter, t = plate thickness.

2.2. Screws

Tapping screws were primarily employed in locations where withdrawal strength was critical (Hu et al., 2022). During installation in the particleboard, caution was exercised to prevent thread stripping. The maximum torque applied to a screw before thread failure in the particle board is defined using equation (3) in accordance with Khurmi and Gupta (2005).

$$T = 3.16 + 0.0069X \quad (3)$$

where T is torque (Nm) and X is the density of the board (kg m^{-3}).

Equation (4) is for 8-gauge screws with a depth of penetration of 15.9 mm. The maximum torque is fairly constant for lead holes of 0% to 90% of the root diameter of the screw.

Ultimate withdrawal loads P (N) of screws from particleboard were predicted using equation (4), given in accordance with the USDA Wood Handbook (2021).

$$P = KD1/2\ (L\text{-}D/3)3/4\ G2 \quad (4)$$

where: D = shank diameter of the screw (mm, in.), L = depth of embedment of the threaded portion of the screw (mm), and G = specific gravity of the board based on oven-dry weight and volume at current moisture content. K = 41.1 for withdrawal from the face of the board and K = 31.8 for withdrawal from the edge. Other screw withdrawal load resistance considerations were in accordance with Hu et al. (2022).

2.3. Cutting force

The cutting force was evaluated following Bershadskiy and Tsvetkova (1975) as cited in Vlasev (2018), with the tangential cutting force subsequently determined using equation (5).

$$P = \frac{kbhU}{v}, N, \quad (5)$$

where P is the tangential force of cutting (N), k is the specific cutting energy in N/mm^2, b is the width of the slot (m), h is the height of the slot (m), U is the feed rate ($m.s^{-1}$), and v is the cutting velocity ($m.s^{-1}$).

3. Resources utilisation and manufacturing feasibility

The materials required for fabricating the APJ were derived from the bill of materials generated by the design software (Fig. 3). The material quantities demonstrate a judicious use of resources, combining a stronger, more sustainable material (*Khaya ivorensis*) for critical components with readily available composite material (MDF) for secondary elements. The corresponding fabrication costs are presented in Table 1, with the total amounting to N15,880.00, equivalent to US$40.89 in 2021. This hybrid approach demonstrates a practical solution for maximising structural performance and long-term durability while maintaining accessibility of materials for local woodworkers.

4. Finite element modelling and simulation

The numerical investigation of the APJ was conducted using SolidWorks Simulation 2021. The jig geometry was discretised using second-order tetrahedral elements (parabolic type), with local mesh refinement at joints and bolt regions to capture potential stress concentrations. The final mesh consisted of approximately 30,000 elements and 45,000 nodes (Fig. 4). A curvature-based mesher with a minimum element size of 2 mm was employed. Mesh quality checks confirmed an average aspect ratio below 1.8 and Jacobian ratio values above 0.6, ensuring numerical accuracy and stability, consistently with practices reported in previous FEM studies (Icha and Odey, 2025).

Table 1. Material Cost Analysis of Tenoning Jig

Description of Item	Qty	Unit	Rate	Amount (N)
MDF	0.5	Half board	17,500	8,750
African Mahogany	1	pieces	1200	1200
Screws	2	pieces	25	50
Medium-size top bond glue	1		800	800
Bolt and nut	4	Pieces	100	400
Washer	5	Pieces	30	180
Transportation				500
Workmanship				4,000
TOTAL				**15,880**

5. Material models

Two types of simulation were evaluated: medium-density fibreboard (MDF) and African mahogany (*Khaya ivorensis*). MDF was included as a structural baseline, since it is widely used in woodworking jigs. Mahogany was introduced to evaluate performance using a stronger option. The material properties (elastic modulus, density, Poisson's ratio and yield strength) were adopted from Hu et al. (2023) for MDF and Icha et al. (2022) for mahogany, and are presented in Tables 2 and 3. Where full orthotropy properties were not available, an isotropic baseline was used for screening, followed by a transversely-orthotropic sensitivity run to bound the response. Both materials were assigned to the entire jig models in separate simulations, with identical boundary conditions, loads and meshing parameters applied to ensure comparability of results.

6. Boundary conditions and loads

The jig base was fully constrained to replicate rigid attachment to the circular saw table. A uniformly distributed load of 470 N was applied to represent the combined effect of workpiece weight and user-applied forces. In addition, concentrated point loads were introduced to simulate clamping and guiding actions (Fig. 4). This magnitude was selected based on experimental observations of operator effort and is confirmed to be an adequate representation of the maximum tangential cutting force (P) calculated using equation (5). This dictates the critical load the jig must withstand during circular saw operations.

7. Contact definition

Contact behaviour between the jig components and the moving workpiece was defined as surface-to-surface with finite sliding. A friction coefficient of 0.33 was applied, following Massaro and Malo (2020), representing a conservative assumption for wood–wood contact conditions.

8. Simulation models and outputs

Two finite element models were developed for this study: a true-scale model, depicting realistic deformation under the applied load (470 N); and a scaled-deformation model, applying amplification factors of 0.0039593 (MDF) and 622.836 (mahogany) to enhance visualisation of stress concentration and possible failure modes, without affecting numerical accuracy. The simulation outputs included von Mises equivalent stress, equivalent elastic strain, total directional deformation, yield strength, and factor of safety (FoS). These parameters were governed by standard continuum mechanics relationships as expressed by Yildirim et al. (2016) in equations (6) to (10) below:

Von Mises stress (σ_{vm})

$$\sigma_{vm} = \sqrt{\frac{1}{2}\left[(\sigma_x - \sigma_y)^2 + (\sigma_y - \sigma_z)^2 + (\sigma_z - \sigma_x)^2\right] + 6(\tau_{xy}^2 + \tau_{yz}^2 + \tau_{zx}^2)} \quad (6)$$

where: σ_x, σ_y, σ_z = normal stresses in the x, y, and z directions, and τ_{xy}, τ_{yz}, τ_{zx} = shear stresses in the respective planes.

Directional deformation (Ui)

$$Ui = \frac{\sigma_i L}{E} \tag{7}$$

where: *Ui* = deformation in direction *i*, σ_i = stress in direction *i*, *L* = initial length of the material, *E* = Young's modulus.

Elastic strain (ε_{vm})

$$\varepsilon_{vm} = \sqrt{\frac{1}{2}\left[(\varepsilon_x - \varepsilon_y)^2 + (\varepsilon_y - \varepsilon_z)^2 + (\varepsilon_z - \varepsilon_x)^2\right] + \frac{3}{4}(\gamma_{xy}^2 + \gamma_{yz}^2 + \gamma_{zx}^2)} \tag{8}$$

where: ε_x, ε_y, ε_z = normal strains in the x, y, and z directions, and $\boldsymbol{\gamma}_{xy}$, $\boldsymbol{\gamma}_{yz}$, $\boldsymbol{\gamma}_{zx}$ = shear strains.

Yield stress (σ_y)

$$\sigma_y = \frac{F_y}{A} \tag{9}$$

where: σ_y = yield stress, F_y = yield force, *A* = cross-sectional area.

Factor of safety (FoS)

$$\text{FoS} = \frac{\sigma_y}{\sigma_{max}} \tag{10}$$

where: σ_y = yield stress, σ_{max} = maximum applied stress.

Table 2. Mechanical properties of MDF used in the study (Hu et al., 2023)

Property	Value	Units
Elastic modulus	70,000	N/m^2
Poisson's Ratio	0.3	N/A
Tensile strength	0.61	N/m^2
Yield strength	2e+07	N/m^2
Mass density	159.99	Kg/m^3
Shear modulus	3e+08	N/m^2

Table 3. Mechanical properties of Khaya ivorensis used in the study (Icha et al., 2022)

Property	Value	Units
Elastic modulus	9.8e+09	N/m^2
Poisson's Ratio	0.032	N/A
Tensile strength	2e+06	N/m^2
Yield strength	3.93e+07	N/m^2
Mass density	600	Kg/m^3
Shear modulus	2.42e+06	N/m^2

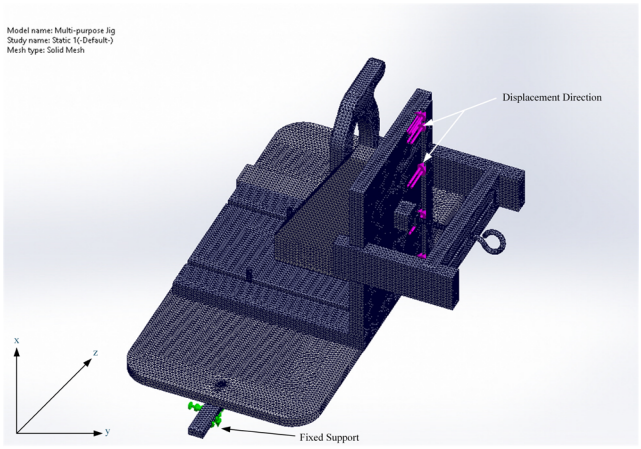


Fig. 4. Mesh and boundary conditions of the all-purpose numerical model

9. Fabrication of APJ

The APJ comprises a base, vertical fence, carriage/slider, clamp block, and handle. Components subjected to cutting and clamping forces were fabricated from mahogany, while MDF was used for non-structural inserts (the base). Materials for the fabrication of the APJ were obtained from the local wood market and processed at the University Wood Products Engineering workshop. A halved-size MDF board and a piece of mahogany plank were cut and machined to the specified design dimensions (Fig. 2). Bolt and knob holes were drilled as detailed, after which the jig was assembled using an electric driver. Screws were inserted perpendicular to the block faces to ensure full thread engagement.

10. Experimental evaluation

Fig. 5 presents the experimental setup of the APJ mounted on the circular saw machine. The applied force was aligned with the rotational direction of the saw blade as it engaged the workpiece. Different types of cuts were processed to assess the jig's precision through visual inspection for vibration, wear and fastener loosening. The jig was further monitored for indications of potential failure, such as crack initiation, bolt loosening, excessive deformation or structural instability, and results were carefully documented. All fastener and load calculations were referenced against standards, including the Forest Products Laboratory General Technical Report (2010) and the USDA Wood Handbook (2021), as detailed in the Design Considerations section.

Results and discussion

1. Simulation analysis of the APJ

Table 3 presents the results of the finite element simulation of the APJs fabricated from MDF and mahogany, respectively. Key performance indicators include von Mises stress, elastic strain, deformation, and factor of safety (FoS). The MDF-based simulation gave a maximum von Mises stress of 1.494×10^8 N/m^2, with an associated maximum strain of 2.722×10^1 and deformation

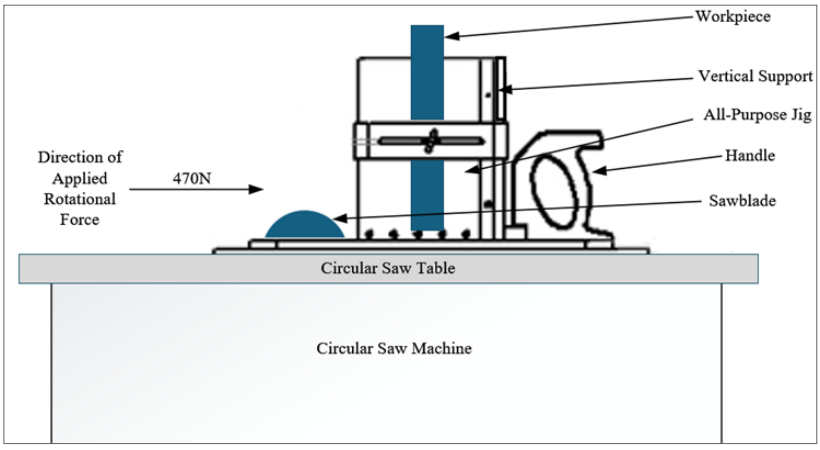


Fig. 5. Experimental setup of the APJ on the circular saw machine

Table 4. Solidworks Simulation results values for MDF and Khaya ivornsis

Object Name	Material	von Mises Stress (N/m²)	Elastic Strain (mm/mm)	Deformation (mm)	Factor of Safety
Max	MDF	1.494×10^{8}	2.722×10^{1}	1.659×10^{4}	2
Min		0.000 x 10	0.000 x 10	0.000 x 10	
Max	Khaya ivornsis	1.130×10^{7}	1.338×10^{-4}	1.052×10^{-1}	12
Min		9.570×10^{-2}	3.920×10^{-13}	0.000 x 10	

of 1.659×10^{4} mm. These values were considered high for the simulated MDF jig, indicating possible numerical instability and structural inadequacy under the applied 470 N load. The FoS for the MDF case was only 2, a marginal value that falls below acceptable design practice for woodworking fixtures. Collectively, although no failure was reported for the MDF, these results suggested that the use of MDF was below suitable sustainable standard; hence, a second simulation was considered using solid wood.

The mahogany-based simulation demonstrated markedly better performance under the same loading conditions. The maximum von Mises stress was 1,130 x 10^{7} N/m², an order of magnitude lower than the value for MDF, with a corresponding maximum strain of 1.338 x 10^{-4}. Deformation was limited to $1.052.10^{-1}$ mm, a value within tolerable limits for precision woodworking. The FoS of 12 indicates a highly reliable structure, with significant reserve strength to withstand normal operator-applied forces without risk of failure. These results highlight mahogany's superior stiffness and strength, which may translate into enhanced dimensional stability and operator safety during saw operations.

2. Load distribution diagrams

Fig. 6(a–c) presents true-scale schematic displacement distribution diagrams for the MDF-based simulated APJ under static loading of 470 N for stress, strain and displacement, respectively. At the applied static load, the von Mises stresses remain relatively low across the jig. However, stress is observed to reach a maximum at the fixed supports of the bar, which slides along the table's slot on loading. As shown in Fig. 6(b), the analyses also reveal that a marginal variation in the stress and strain results is evident at equivalent loading conditions, indicating a slight deviation in the material's response to elastic strain relative to static strain, which implies a minimal impact on structural integrity. Elastic strain is within a range of 1.00×10^{-3} to 2.772×10^{1}, reaching

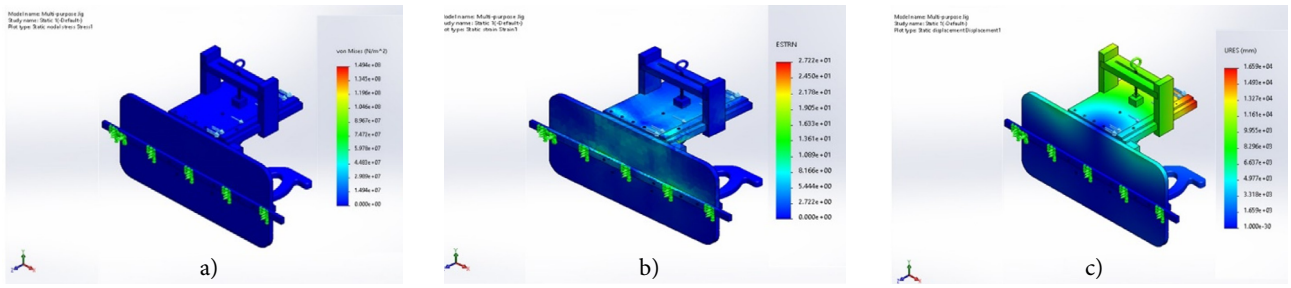


Fig. 6. True scale stress (a), strain (b), and deformation (c). Distribution diagrams for the simulated MDF jig under 470 N load

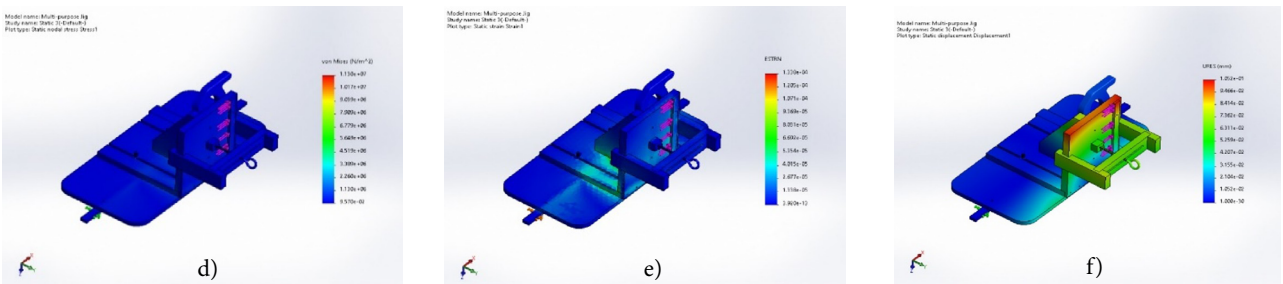


Fig. 7. True scale stress (a), strain (b), and deformation (c). Distribution diagrams for the simulated African mahogany jig under 470 N load

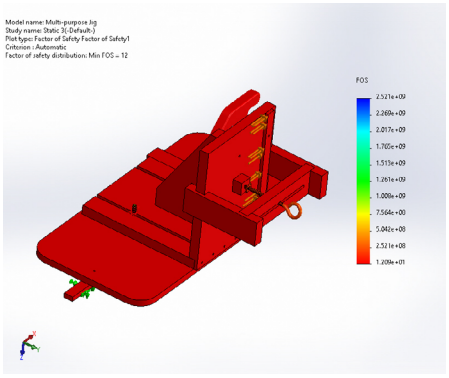


Fig. 8. Factor of safety for the simulated African mahogany APJ at 470 N load

a maximum around the base of the sliding main table and the vertical work support face area. The displacement is highest at the vertical work support area and the adjustable stop bar, at about 1.659 x 10^4 mm, with a relatively lower displacement value in other areas.

Fig. 7(a–c) illustrates the response to stress, strain and displacement of the APJ fabricated from mahogany, subjected to the operational load of 470 N. The simulation reveals a von Mises stress distribution ranging from 9.570 x 10^{-2} to 1.130 x 10^7, indicating exceptionally low stress levels. Peak stress is localised at the vertical work-support base, which engages with the table slot. Despite this concentration, the values remain negligible, affirming mahogany's structural adequacy and reliability for precision jig applications. In turn, the elastic strain analysis shows values for the mahogany APJ ranging from 1.392 ×10^{-13} to 1.33 × 10^{-4}, indicating limited deformation under the 470 N load. The maximum strain is observed to correspond with areas of maximum stress. Overall, the distribution pattern demonstrates consistent structural response, with strain values remaining well within the elastic behaviour range across the jig's geometry. The analysis reveals that the APJ under a load of 470 N exhibits minimal displacement (1.052 x 10^{-1} mm) concentrated in the clamping guiding regions, while the jig's base exhibits negligible displacement (0 mm). These values result in a high factor of safety value of 12 for mahogany, indicating a lower risk of failure under the specified load conditions. In comparison, MDF has a factor of safety of 2, highlighting mahogany's superior structural performance due to its higher stiffness and strength.

3. Failure modes of the APJ

Fig. 9(a–f) presents the simulated failure modes of the APJ when fabricated from MDF and African mahogany, with scaling factors applied to deformation to enhance visualisation. Fig. 9(a–c) represents the MDF case at a scale factor of 0.0039593. The MDF jig exhibited highly localised stress concentrations, particularly around the clamping and joint regions (Fig. 9a). The corresponding strain distribution (Fig. 9b) showed widespread zones of elevated elastic strain, indicating low resistance across the structure. Displacement fields (Fig. 9c) confirmed excessive deflection. This minimal scaling factor (0.0039593) was necessitated because the model predicted a structural deformation so large that visualisation required a significant downscaling factor, underscoring the structural collapse of the MDF-only

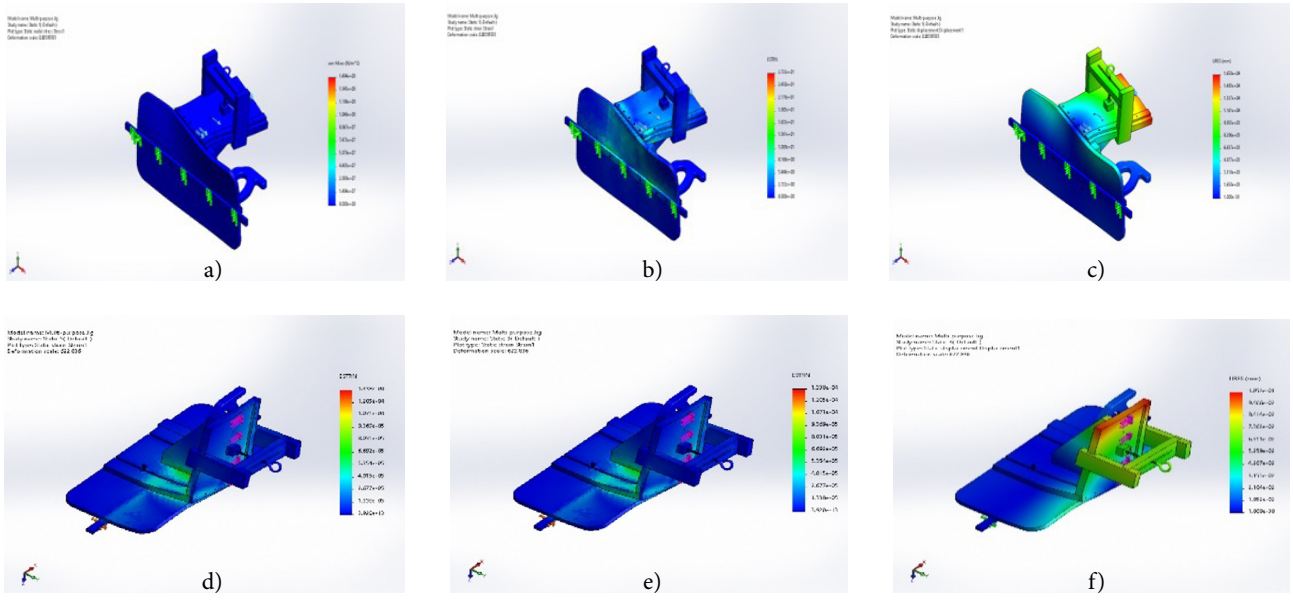


Fig. 9. Failure mode distribution diagrams of the APJ: (a–c) MDF scaled at 0.0039593, showing von Mises stress (a), elastic strain (b), displacement (c); (d–f) African Mahogany scaled at 622.836, showing von Mises stress (d), elastic strain (e), displacement (f)

design under operational load. In turn, African mahogany displayed similar failure modes (Fig. 9d–f), but at a high amplification scale of 622.836. The extreme difference between the amplification factors for the MDF and mahogany highlights the differences in structural integrity between the materials. However, it should be noted that neither of these materials failed in their true scales; amplification was applied to enhance the visualisation of stress concentration and possible failure modes.

4. Fabrication and empirical evaluation of the APJ

Based on the numerical simulation results, which indicated excessive deformation and poor safety margins when MDF was used alone, material modifications were introduced at the prototype fabrication stage. The final design incorporated a hybrid configuration of MDF and mahogany, combining the dimensional stability and machinability of MDF with the superior stiffness and strength of mahogany. Critical load-bearing and guiding elements, such as the vertical support and clamping arms, were fabricated from mahogany to withstand operational stresses, while secondary structural components were built from MDF to reduce weight and material cost.

The fabrication of the all-purpose jig (Fig. 10) was evaluated for functionality, safety and ease of operation. Fabrication was achieved using standard hand and portable tools, with the improvised knobs for fastening bolts particularly effective in facilitating quick adjustment and secure tightening during use. The jig was mounted on the circular saw machine in the university departmental workshop and applied in a series of cutting operations, serving to make tongues and grooves, tenons and others. Representative samples of workpieces processed with the jig are presented in Fig. 11, confirming its adaptability across different woodworking tasks.

During testing, the jig was observed to maintain stability and alignment with minimal vibration, ensuring accurate cuts and reducing the risk of operator error.



Fig. 10. All-purpose jig mounted for evaluation on the circular saw machine



Fig. 11. Samples of cuts and grooves produced using the APJ on the circular saw machine

No structural failure such as cracking, fastener loosening or joint deformation was recorded, demonstrating that the design could withstand the operational loads applied. The overall performance showed that the jig improved both the efficiency and safety of the woodworking process, offering woodworkers a reliable, versatile and affordable accessory for enhancing the functionality of the circular saw machine. These observations agree with earlier work by DeCristoforo (1988), Capototos (1983), and Icha and Odey (2024).

Conclusions

This study investigated the performance and failure behaviour of an all-purpose jig for circular saw operations through finite element modelling, simulation and fabrication. Two materials were assessed numerically: medium-density fibreboard (MDF) and African mahogany (*Khaya ivorensis*). Simulation results showed that the MDF jig experienced higher stresses, strain and deformations than the African mahogany jig. The failure mode, though similar, demonstrated that mahogany has superior stiffness and reliability under the applied load. Based on these findings, a prototype was fabricated, combining mahogany in critical load-bearing components with MDF in non-critical parts. This design achieved a balance of structural performance, making it suitable for practical use in woodworking workshops. The APJ improves the usability and safety of circular saw machines. The developed model enhances operator safety and offers a verifiable foundation for improving the structural reliability and durability of locally produced jigs. Beyond its practical applications, this study contributes to the growing body of knowledge on integrating finite element modelling into woodworking design optimisation, especially for resource-constrained settings. Further long-term validation in industrial environments would be valuable to fully assess wear, fatigue and environmental stability over extended operational periods.

Conflict of interest

The author(s) declare(s) that there is no conflict of interest concerning the publication of this article.

References

Amid, N. H. C., Abd Rahman, Z., Rohimi, R., Mohamed, S. B., Kasim, M. S., Mohamad, W. N. F. W., ... & Maharof, M. (2025). Design and Development of a Universal Magnetic Portable Jig: A Modular Approach for Versatile Clamping Applications. Journal of Advanced Research Design, 125(1), 79-102. https://doi.org/10.37934/ard.125.1.79102

Autengruber, M., Lukacevic, M., Wenighofer G., Raimund Mauritz, R., & Füssl, J. (2021). Finite-element-based concept to predict stiffness, strength, and failure of wood composite I-joist beams under various loads and climatic conditions. Engineering Structures, 245 112908, DOI: 10.1016/j.engstruct.2021.112908

Blomqvist, L., Ormarsson, S. & Ziethén, R. (2023). Stress distribution in veneers under lamination and simultaneously bending: an experimental and numerical investigation. Wood Material Science & Engineering, 18:3, 995-1002, DOI:10.1080/17480272.2022.2099762

DeCristoforo, R.J. (1988). The Complete Book of Stationary Power Tool Techniques. Sterling Publishing Co., Inc. Two Park Avenue, New York, N. Y. 388p

Falko, F. Ehrenstein, J. Höltgen, C. Blondrath, A. Schäper, L. Göppert, A. & Schmitt, R. (2023). Jigs and fixtures in production: a systematic literature review. Journal of Manufacturing Systems, 72, 373–405, DOI: 10.1016/j.jmsy.2023.10.006

Frontini F. (2023) A novel approach for modelling a historic timber roof. International Wood Products Journal, 14:1, 21-33, DOI: 10.1080/20426445.2023.2171895

Heisel, U., Stehle, T., & Ghassemi, H. (2014). A simulation model for analysis of roll tensioning of circular saw blade. Advanced Materials Research, 1018, 57-66. doi:10.4028/www.scientific.net/AMR.1018.57

Hong, J. P., & Barrett, D. (2010). Three-dimensional finite-element modelling of nailed connections in wood. Journal of Structural Engineering, 136(6), 715-722. DOI: 10.1061/ASCEST.1943-541X.0000160

Huber, J. A., Broman, O., Ekevad, M., Oja, J., & Hansson, L. (2022). A method for generating finite element models of wood boards from X-ray computed tomography scans. Computers & Structures, 260, 106702, DOI: 10.1016/j.compstruc.2021.106702

Hu, W., Yan Liu Y., & Konukcu, A. C. (2022). Study on withdrawal load resistance of screw in wood-based materials: experimental and numerical. Wood Material Science & Engineering, DOI: 10.1080/17480272.2022.2084699

Icha, A. A., & Odey, S. O. (2024). Development of a master jig for circular saw machine. Nigerian Journal of Engineering Research Unicross (NJERU) ISSN No. 2971-785X 1(2), 87-95. https://njerunicross.com.ng/assets/images/articles/1727797215_article.pdf

Icha, A. A., & Odey, S. O. (2024). Modelling and simulation of a tenoning jig to predict performance and failure mode on circular saw machine. International Wood Products Journal, 15(1), 44–54. DOI: 10.1177/20426445241226534

Icha, A.A., & Odey S.O. (2025). Performance and deformation behavior of a master jig on circular saw machine using finite element method. Furniture and Wooden Material Research Journal, 8 (1), 143-155, DOI: 10.33725/mamad.1663809

Icha, A. A., & Odey, S. O. (2024). Modelling and simulation of a tenoning jig to predict performance and failure mode on circular saw machine. International Wood Products Journal, 15(1), 44–54. DOI: 10.1177/20426445241226534

Icha A, Odey S, Ekpe H (2024) A finite element approach to ınvestigate the performance and reliability of an extension stand in table saw machines. Wood Industry and Engineering, 6(2),1-13. https://dergipark.org.tr/en/pub/wie/issue/89190/1503930

Kumar, D. R., Samui, P., Burman, A., Wipulanusat, W., & Keawsawasvong, S. (2023). Liquefaction susceptibility using machine learning based on SPT data. Intelligent Systems with Applications, 20, 200281. https://doi.org/10.1016/j.iswa.2023.200281

Kumar, S. R., Campilho, R. D. S. G., & Silva, F. J. G. (2019). Rethinking modular jigs' design regarding the optimization of machining times. Procedia Manufacturing, 38, 876–883. DOI: 10.1016/j.promfg.2020.01.169

Li, B., Zhang, Z., Li, W., & Peng, X. (2015). A numerical simulation on multi-spot pressure tensioning process of circular saw blade. Journal of Wood Science, 61(6), 578-585. DOI:10.1007/s10086-015-1508-5

Marinkovic, D., & Zehn, M. (2019). Survey of finite element method-based real-time simulations. Applied Sciences, 9(14), 2775. https://doi.org/10.3390/app9142775

Massaro, F. M., & Malo, K. A. (2020). Stress-laminated timber decks in bridges: Friction between lamellas, butt joints and pre-stressing system. Engineering Structures, 213, 110592, ISSN 0141-0296, DOI: 10.1016/j.engstruct.2020.110592

Miller, A. S., & Hannam, R. G. (1985). Computer aided design using a knowledge base approach and its application to the design of jigs and fixtures. Proceedings of the Institution of Mechanical Engineers, Part B: Management and engineering manufacture, 199(4), 227-234

Nanthakumar, K., & Prabakaran, V. (2014). Design and fabrication testing of combined multipurpose jig and fixture. IOSR Journal of Mechanical and Civil Engineering. www.iosrjournals.org

Odey, S. O., & Icha, A. A. (2022). Finite element modelling and evaluation of a sliding table jig for mitering operations in circular saw machine. Journal of Contemporary Research (JOCRES) 1(2), 173-181. ISSN: 2814-2241

Okpala, C. C., & Okechukwu, E. (2015). The design and need for jigs and fixtures in manufacturing. Science Research, 3(4), 213-219. doi:10.11648/j.sr.20150304.19

Pethe, D., Borkar, V., Gupta, R., Deotale, V., Choudhari, V., & Ganorkar, A. B. (2019). Productivity improvement in priming shop by using jig and fixture. International Journal for Research in Applied Science and Engineering Technology, 7(3), 178-181. http://doi.org/10.22214/ijraset.2019.3029

Radhwan, H., Effendi, M. S. M., Rosli, F.R., Shayfull, Z. & Nadia, K. N. (2019). Design and analysis of jigs and fixtures for manufacturing process. IOP Conference Series Materials Science and Engineering, 551(1), 012028–012028, DOI:10.1088/1757-899x/551/1/012028

Said, N. A., Roslan, M. A., Ngah, N., Mohamad, A. J., Roslan, U. N., Mamat, R. M. R., ... & Yusof, M. F. A. (2023). Design and fabrication of jig and fixture for drilling machine in the manufacturing industry to improve time productivity. Journal of Advanced Research in Applied Sciences and Engineering Technology, 29(2), 304-313. https://doi.org/10.37934/araset.29.2.304313

Salin, J. G. (2008). Modelling water absorption in wood. Wood Material Science and Engineering, 3(3-4), 102-108. DOI: 10.1080/17480270902781576

Seward, D. (2014). Connections. In: Understanding Structures. Palgrave, London. 231-251, DOI: 10.1007/978-1-349-14809-7_10

SOLIDWORKS. (2021). SolidWorks 2021 [Computer software]. Dassault Systèmes

Szabó, B., & Babuška, I. (2021). Finite element analysis: Method, verification and validation.

Vassiliou, V., Barboutis, I., & Kamperidou, V. (2016). Strength of corner and middle joints of upholstered furniture frames constructed with black locust and beech wood. Wood Res, 61(3), 495-504

Yıldırım, M. N, Karaman, A., & Akınay, A. (2016). Finite element method application of wooden furniture. International conference on research in education science, Bodrum/Muğla/Türkiye, 19–22 May 2016, 1258-1270

Zhong, W., Zhang, Z., Chen, X., Wei, Q., Chen, G., & Huang, X. (2021). Multi-scale finite element simulation on large deformation behavior of wood under axial and transverse compression conditions. Acta Mechanica Sinica, 37, 1136-1151, DOI: 10.1007/s10409-021-01112-z